

Rat pial microvascular responses to melatonin during bilateral common carotid artery occlusion and reperfusion

Abstract: The present study assessed the *in vivo* rat pial microvascular responses induced by melatonin during brain hypoperfusion and reperfusion (RE) injury. Pial microcirculation of male Wistar rats was visualized by fluorescence microscopy through a closed cranial window. Hypoperfusion was induced by bilateral common carotid artery occlusion (BCCAO, 30 min); thereafter, pial microcirculation was observed for 60 min. Arteriolar diameter, permeability increase, leukocyte adhesion to venular walls, perfused capillary length (PCL), and capillary red blood cell velocity (V_{RBC}) were investigated by computerized methods. Melatonin (0.5, 1, 2 mg/kg b.w.) was intravenously administered 10 min before BCCAO and at the beginning of RE. Pial arterioles were classified in five orders according to diameter, length, and branchings. In control group, BCCAO caused decrease in order 2 arteriole diameter (by $17.5 \pm 3.0\%$ of baseline) that was reduced by $11.8 \pm 1.2\%$ of baseline at the end of RE, accompanied by marked leakage and leukocyte adhesion. PCL and capillary V_{RBC} decreased. At the end of BCCAO, melatonin highest dosage caused order 2 arteriole diameter reduction by $4.6 \pm 2.0\%$ of baseline. At RE, melatonin at the lower dosages caused different arteriolar responses. The highest dosage caused dilation in order 2 arteriole by $8.0 \pm 1.5\%$ of baseline, preventing leakage and leukocyte adhesion, while PCL and V_{RBC} increased. Luzindole (4 mg/kg b.w.) prior to melatonin caused order 2 arteriole constriction by $12.0 \pm 1.5\%$ of baseline at RE, while leakage, leukocyte adhesion, PCL and V_{RBC} were not affected. Prazosin (1 mg/kg b.w.) prior to melatonin did not significantly change melatonin's effects. In conclusion, melatonin caused different responses during hypoperfusion and RE, modulating pial arteriolar tone likely by MT1 and MT2 melatonin receptors while preventing blood–brain barrier changes through its free radical scavenging action.

Introduction

Melatonin, an indoleamine synthesized in the pineal gland during the dark period in all mammalian species, has been shown to exert potent antioxidant activity [1, 2]. Both *in vitro* and *in vivo* studies indicate that melatonin protects cells and tissues against oxidative damage induced by free radical-generating agents [3–5]. Several studies demonstrated that melatonin scavenges hydroxyl and peroxy radicals and is a more potent antioxidant than vitamin E, mannitol, and glutathione [1, 6–9]. Manev and Uz [10] reported that pinealectomized rats are vulnerable to kainate-induced excitotoxicity and photothrombotic brain injury [9]. Moreover, recent studies have reported beneficial effects exerted by melatonin against cerebral global and focal ischemia–reperfusion (RE) injury [11–14].

Melatonin exerts receptor-mediated effects at physiological concentrations, whereas the receptor-independent actions can be achieved by both physiological and pharmacological concentrations [15]. Two melatonin receptors,

Dominga Lapi¹, Sabrina Vagnani², Emilio Cardaci³, Marco Paterni⁴ and Antonio Colantuoni¹

¹Department of Neuroscience, 'Federico II' University Medical School, Naples, Italy; ²Division of General Surgery and Transplants, Department of Oncology, Transplants and Advanced Technologies in Medicine, University of Pisa, Pisa, Italy; ³Department of Physiological Sciences, 'G. Moruzzi' University of Pisa, Pisa, Italy; ⁴CNR Institute of Clinical Physiology, Pisa, Italy

Key words: arteriolar tone, bilateral common carotid artery occlusion, melatonin, MT1, MT2, and MT3 melatonin receptors, pial microcirculation, radical oxygen species, reperfusion

Address reprint requests to Dominga Lapi, PhD, Department of Neuroscience, 'Federico II' University Medical School, Via S. Pansini, 5, 80121 Naples, Italy.
E-mail: d.lapi@dfb.unipi.it

Received November 12, 2010;
Accepted February 18, 2011.

MT1 and MT2, belonging to the G-protein-coupled receptor superfamily, have been cloned in mammals and share some specific short amino acid sequences, suggesting that they represent a specific subfamily. A third melatonin-binding site has been purified and characterized as the enzyme quinone reductase 2 (MT3); the inhibition of this enzyme by melatonin may contribute to its anti-oxidative properties [16, 17].

In vivo experimental studies observed that melatonin causes constriction of rat cerebral arterioles and facilitates the cerebral blood flow autoregulation, suggesting that melatonin may diminish the risk of hypoperfusion-induced cerebral ischemia [18]. Moreover, melatonin increases the cerebrovascular capacity by constriction of the large cerebral influx arteries. The *in vitro* melatonin-induced constriction of large-diameter cerebral arteries is triggered by G protein-dependent inhibition of Ca^{2+} -activated large-conductance K^+ channels (BK_{Ca}) [19, 20].

In contrast, few data have been reported on melatonin's effects on small diameter cerebral arterioles mainly involved in cerebral blood flow autoregulation. Today,

the molecular mechanisms underlying the effects of melatonin on pial microcirculation have not been completely clarified.

The present study investigated the *in vivo* pial microvascular responses induced by melatonin during brain hypoperfusion and RE injury induced by transient bilateral common carotid artery occlusion (BCCAO) in the rat. Furthermore, we assessed the diameter changes of pial arterioles caused by different doses of melatonin, and we evaluated the effect on pial arteriolar diameter by MT1, MT2, and MT3 melatonin receptor inhibition under baseline and hypoperfusion conditions.

Materials and methods

Experimental groups

The study was carried out in male Wistar rats weighing 250–300 g (Harlan, Italy) randomly assigned to the following groups: (i) Sham-operated rats (group SO, n = 11) subjected to the same procedures as the experimental groups except for the BCCAO; (ii) Control rats (group C, n = 15) were treated with 1.5-mL vehicle (physiological saline solution containing 4% ethanol), intravenously (i.v.) injected, and subjected to 30 min of BCCAO and 60 min of RE; (iii) The third group (subgroup Ma, n = 15; subgroup Mb, n = 15; subgroup Mc, n = 15) was treated with i.v. melatonin, 0.5, 1.0, and 2.0 mg/kg body weight (b.w.), respectively, and infused in 3, 10 min before BCCAO, and at the beginning of RE; (iv) The fourth group (subgroup LMcl, n = 15 subgroup

LMc2, n = 15) was treated with i.v. luzindole, a specific inhibitor of MT2 melatonin receptors and a specific inhibitor of MT1 melatonin receptors, at dosage of 2.0 and 4.0 mg/kg b.w., respectively. Luzindole was infused prior to the highest dose of melatonin and administered 10 min before BCCAO and at the beginning of RE; (v) The fifth group of rats (PMc, n = 15) was treated with i.v. prazosin, specific inhibitor of MT3 melatonin receptors, at dosage of 1.0 mg/kg b.w., infused prior to the highest dose of melatonin, and administered 10 min before BCCAO and at the beginning of RE. In groups SO, C, Ma, Mb, Mc, LMcl, LMc2, and PMc, three of 15 rats were treated with artificial cerebrospinal fluid (aCSF) containing 250.0 mM 2'-7'-dichlorofluorescein-diacetate (DCFH-DA) during BCCAO and three animals at RE. (vi) The sixth group of rats (subgroups L1, L2, and P group, n = 9, respectively) was subjected to i.v. administration of luzindole (2.0 and 4.0 mg/kg b.w.) or prazosin (1.0 mg/kg b.w.) 10 min before BCCAO and the beginning of RE. (vii) Finally, the last group of animals was treated with melatonin (0.5 mg/kg b.w., 1.0 mg/kg b.w. and 2.0 mg/kg b.w., n = 5 for each dose) or luzindole (2.0 mg/kg b.w., 4.0 mg/kg b.w., n = 5 for each dose) or prazosin (1.0 mg/kg b.w., n = 5) without BCCAO and RE.

In pilot experiments, we examined the effects of luzindole and prazosin at the different doses administered prior to melatonin treatment (2.0 mg/kg b.w.). Based in the outcome of these studies, we did not observe significant changes when compared with LMcl, LMc2, and PMc groups (Table 1).

Table 1. Drug treatment (T): doses, route, and time of administration in the different experimental groups

Group	H/R plus T	Time	N	Group	NO H/R plus T	Time	N
C	Saline solution 1.5 mL i.v.	Prior BCCAO At Reperfusion beginning	15	SO	Saline solution 1.5 mL i.v.	Twice at 50-min interval	11
Ma	Melatonin 0.5 mg/kg b.w. i.v.	Prior BCCAO At R beginning	15	ma	Melatonin 0.5 mg/kg b.w. i.v.	Twice at 50-min interval	5
Mb	Melatonin 1.0 mg/kg b.w. i.v.	Prior BCCAO At R beginning	15	mb	Melatonin 1.0 mg/kg b.w. i.v.	Twice at 50-min interval	5
Mc	Melatonin 2.0 mg/kg b.w. i.v.	Prior BCCAO At R beginning	15	mc	Melatonin 2.0 mg/kg b.w. i.v.	Twice at 50-min interval	5
LMcl	Luzindole 2.0 mg/kg b.w. i.v.	Prior Melatonin	15	l ₁	Luzindole 2.0 mg/kg b.w. i.v.	Twice at 50-min interval	5
LMc2	Melatonin 2.0 mg/kg b.w. i.v.	Prior BCCAO At R beginning	15	l ₂	Luzindole 4.0 mg/kg b.w. i.v.	Twice at 50-min interval	5
	Luzindole 4.0 mg/kg b.w. i.v.	Prior Melatonin					
PMc	Melatonin 2.0 mg/kg b.w. i.v.	Prior BCCAO At R beginning	15	p	Prazosin 1.0 mg/kg b.w. i.v.	Twice at 50-min interval	5
	Prazosin 1.0 mg/kg b.w. i.v.	Prior Melatonin					
L1	Luzindole 2.0 mg/kg b.w. i.v.	Prior BCCAO At R beginning	9				
L2	Luzindole 4.0 mg/kg b.w. i.v.	Prior BCCAO At R beginning	9				
P	Prazosin 1.0 mg/kg b.w. i.v.	Prior BCCAO At R beginning	9				

H/R, animals subjected to hypoperfusion and reperfusion and NO H/R animals not subjected to hypoperfusion and reperfusion; N, number of rats utilized; BCCAO, bilateral common carotid artery occlusion.

Administration of drugs

Melatonin solutions were prepared by dissolving 0.5, 1.0, and 2.0 mg/kg b.w. in 0.5 mL of saline solution containing 4% ethanol and i.v. infused (3 min) to the rats 10 min before BCCAO and at the beginning of RE.

Luzindole (2.0 and 4.0 mg/kg b.w.) and prazosin (1.0 mg/kg b.w.) were dissolved in 0.5 mL of saline solution, respectively. Each substance was i.v. administered 10 min prior to melatonin (2.0 mg/kg b.w.).

2'-7'-Dichlorofluorescein-diacetate was mixed with aCSF to obtain a concentration of 250.0 μ M. This solution was superfused over the pial surface for 15 min during ischemia or at RE.

These drugs were purchased from Sigma Chemical, St. Louis, MO, USA.

Animal surgical preparation

Anaesthesia was induced with α chloralose (50.0 mg/kg b.w., i.p.) plus urethane (600.0 mg/kg body weight, i.p.) and maintained with urethane (100.0 mg/kg b.w., i.v. every hour). Rats were tracheotomized, paralyzed with tubocurarine chloride (1.0 mg/kg h, i.v.), and mechanically ventilated with room air and supplemental oxygen. The right and left common carotid arteries were isolated for successive clamping. A catheter was placed in the left femoral artery for arterial blood pressure recording and blood gases sampling. Another catheter was placed in the right femoral vein for the fluorescent tracer injection [fluorescein isothiocyanate bound to dextran, molecular weight 70 kDa (FD 70), 50 mg/100 g b.w., i.v. as 5.0% wt/vol solution in 3 min administered just once at the beginning of experiment after 30 min of the preparation stabilization; rhodamine 6G, 1.0 mg/100 g b.w. in 0.3 mL, as a bolus with supplemental injection throughout BCCAO and RE (final volume 0.3 mL/100 g/h) to label leukocytes for adhesion evaluation] and for drug administration. Blood gas measurements were carried out on arterial blood samples withdrawn from arterial catheter at 30-min time period intervals (ABL5; Radiometer, Copenhagen, Denmark). Throughout all experiments, mean arterial blood pressure (MABP), heart rate, respiratory CO₂, and blood gases values were recorded and maintained stable within physiological ranges. Rectal temperature was monitored and preserved at 37.0 \pm 0.5°C with a heating stereotaxic frame where the rats were secured.

A closed cranial window (4 \times 5 mm) was implanted above the left frontoparietal cortex (posterior 1.5 mm to bregma; lateral, 3 mm to the midline) to observe the pial microcirculation [21]. To prevent overheating of the cerebral cortex during drilling, cold saline solution was suffused on the skull. The dura mater was gently removed and a 150 μ m-thick-quartz microscope cover glass was sealed to the bone with dental cement. The window inflow and outflow were assured by two needles secured in the dental cement of the window, so that the brain parenchyma was continuously superfused with aCSF [22, 23]. The rate of superfusion was 0.5 mL/min controlled by a peristaltic pump. During superfusion, the intracranial pressure was maintained at 5 \pm 1 mmHg and measured by a pressure

transducer connected to a computer. The composition of the aCSF was as follows: 119.0 mM NaCl, 2.5 mM KCl, 1.3 mM MgSO₄·7H₂O, 1.0 mM NaH₂PO₄, 26.2 mM NaHCO₃, 2.5 mM CaCl₂, and 11.0 mM glucose (equilibrated with 10.0% O₂, 6.0% CO₂, and 84.0% N₂; pH 7.38 \pm 0.02). The temperature was maintained at 37.0 \pm 0.5°C [24].

Cerebral blood flow reduction was produced by placement of two atraumatic microvascular clips for 30 min on common carotid arteries, previously isolated. After clamp removing, the pial microcirculation was observed for 60 min (RE period).

The experiments were carried out in the morning from 08.00 am to 02.00 pm, with at least two animals studied per day, with random distribution for the different experimental groups.

All experiments conformed to the *Guide for the Care and Use of Laboratory Animals* published by the US National Institutes of Health (NIH Publication No. 85-23, revised 1996) and to institutional rules for the care and handling of experimental animals. This procedure provides that all animals were euthanized at the end of the experimental procedure by pentobarbital overdose intravenously administered. The protocol was approved by the 'Federico II' University of Naples Ethical Committee.

Intravital microscopy

Pial vessels were observed using a fluorescence microscope (Leitz Orthoplan, Wetzlar, Germany) fitted with long-distance objectives [2.5 \times , numerical aperture (NA) 0.08; 10 \times , NA 0.20; 20 \times , NA 0.25; 32 \times , NA 0.40], a 10 \times eyepiece, and a filter block (Ploemopak, Leitz). Epi-illumination was provided by a 100-W mercury lamp using the appropriate filters for FITC or rhodamine 6G and a heat filter (Leitz KG1). The pial microcirculation was televised with a DAGE MTI 300RC low-light level digital camera and recorded by a computer-based frame grabber (Pinnacle DC 10 plus; Avid Technology, MA, USA).

Microvascular measurements were made off-line using a computer-assisted imaging software system (MIP Image; CNR, Institute of Clinical Physiology, Pisa, Italy). The visualization of pial microcirculation was performed for 1 min every 5 min during substance administration and at the beginning of RE (20 min). Afterwards, recording was carried out every 10 min during BCCAO and the remaining RE (Fig. 1). Because of homogeneous responses during different experiments, we chose to report data collected under baseline conditions, at the end of BCCAO and the end of RE.

Microvascular parameter evaluation

Under baseline conditions, the arteriolar network was mapped by stop-frame images and pial arterioles were classified according to a centripetal ordering scheme (Strahler's method, modified according to diameter), as previously described [25]. In each animal, two order 4 arterioles, two order 3, and two order 2 arterioles were studied during each experiment. We do not report the results related to order 5 and order 1 arterioles because the

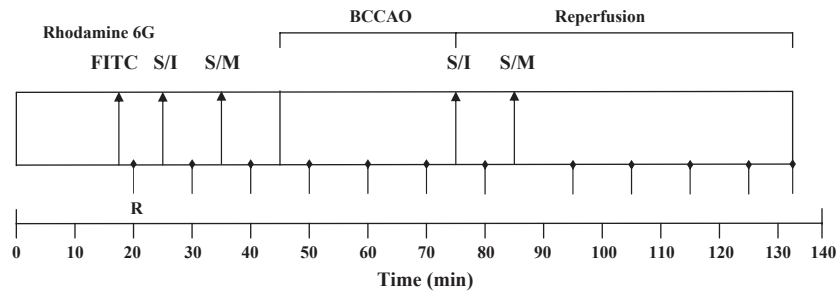


Fig. 1. Experimental design of drug administration and measurement times. R, recording points; FITC, fluorescent-dextran (70 kDa) and rhodamine 6G; S/I, saline solution containing 4% ethanol and/or melatonin receptor inhibitor administration (luzindole, prazosin); S/M, saline solution containing 4% ethanol and/or melatonin administration; BCCAO, bilateral common carotid artery occlusion. Rhodamine 6G was injected after FITC-dextran as a bolus and then infused during BCCAO and reperfusion.

large arterioles were located to the peripheral of the cranial window while the small arterioles penetrated in the cortex.

Arteriolar diameters were measured with a computer-assisted method (frame by frame). The results of diameter measurements were in agreement with those obtained by shearing method ($\pm 0.5 \mu\text{m}$). The increase in permeability was calculated and reported as normalized grey levels (NGL): $\text{NGL} = (I - I_r)/I_r$, where I_r is the average baseline grey level at the end of vessel filling with fluorescence (average of five windows located outside the blood vessels with the same windows being used throughout the experimental procedure), and I is the same parameter at the end of BCCAO or RE. Grey levels ranging from 0 to 255 were determined by the MIP Image program in five regions of interest (ROI) measuring $50 \times 50 \mu\text{m}$ ($10\times$ objective). The same location of ROI during recordings along the microvascular networks was provided by a computer-assisted device for XY movement of the microscope table.

Adherent leukocytes (i.e., cells on vessel walls that did not move over a 30-s observation period) were quantified in terms of number/ $100 \mu\text{m}$ of venular length (v.l.)/30 s using higher magnification ($10\times$, $20\times$, and $32\times$ microscope objectives). In each experimental group, 45 venules were studied.

Perfused capillary length (PCL) was measured by MIP image in an area of $150 \times 150 \mu\text{m}$. In this system, the length of perfused capillaries is easily established by the automated process because it is outlined by dextran. [26].

The capillary red blood cell velocity (V_{RBC}) was measured with a computer-assisted method (frame by frame). To avoid bias because of single operator measurements, the quantification of all microvascular parameters were made by two independent 'blinded' operators. Their measurements overlapped in all cases.

Analysis of rhythmic diameter changes

All diameter time series were analyzed by temporal and frequency domains under basal conditions, during BCCAO and at RE. Data analysis programs were written using MATLAB (Mathworks Inc., Natick, MA, USA).

The Lomb–Scargle method was used to estimate the power spectral density of the diameter time series [27]. This spectral estimation method has been specifically developed to manage unevenly time-spaced data series. Although

interpolation appears to be the easier way to obtain evenly spaced data from unevenly spaced data, as long gaps are present, these can produce spectra with spurious bulge of power at low frequencies. The Lomb–Scargle method mitigates these biases because it evaluates data only at times actually measured and it weights data on a 'per point' instead of a 'per time interval' basis; this explains its better performance compared to fast Fourier transform in the unevenly spaced data cases.

Reactive oxygen species quantification

Artificial cerebrospinal fluid containing 250.0 mM DCFH-DA at $37.0 \pm 0.5^\circ\text{C}$ was superfused over the pial surface. The lipophilic DCFH-DA is a stable nonfluorescent probe with a high cellular permeability. DCFH-DA reacts with intracellular radicals to be converted to its fluorescent product (DCF). The remaining extracellular DCFH-DA was washed out with aCSF. The intensity of DCF fluorescence is proportional to the intracellular radical oxygen species (ROS) level.

The fluorescence intensity was determined by the use of an appropriate filter (522 nm) and the evaluation of NGL, with the baseline represented by pial surface just superfused by DCFH-DA [28].

Physiological parameters recording

Mean arterial blood pressure (Viggo-Spectramed P10E2 transducer, Oxnard, CA, USA, connected to a catheter in the femoral artery) and heart rate were monitored with a Gould Windograf recorder (model 13-6615-10S, Gould, OH, USA). Data were recorded and stored in a computer. Blood gas measurements were carried out on arterial blood samples withdrawn from arterial catheter at 30-min time period intervals (ABL5; Radiometer, Copenhagen, Denmark). The hematocrit was measured under baseline conditions, at the end of BCCAO and at RE.

Statistical analysis

All reported values are means \pm S.D. Data were tested for normal distribution with the Kolmogorov–Smirnov (KS) test. Parametric (Student's t tests, ANOVA, and Bonfer-

roni post hoc test) or nonparametric tests (Wilcoxon, Mann–Whitney and Kruskal–Wallis tests) were used. Nonparametric tests were applied to compare diameter and length data among experimental groups because KS test indicated non-Gaussian distribution of data.

The statistical analysis was carried out by SPSS 14.0 statistical package. Statistical significance was set at $P < 0.05$.

Results

Pial arterioles were classified according to diameter, length, and branching. Capillaries were assigned order 0 and the arterioles were assigned order 1–5 according to their branching. Order 5 showed a mean diameter of $63.0 \pm 4.5 \mu\text{m}$ and mean length of $1172 \pm 400 \mu\text{m}$, $n = 74$; order 4: mean diameter $45.5 \pm 4.0 \mu\text{m}$ and mean length $980 \pm 220 \mu\text{m}$, $n = 198$; order 3: mean diameter $34.5 \pm 3.0 \mu\text{m}$ and mean length $485 \pm 105 \mu\text{m}$, $n = 210$; order 2: mean diameter $25.0 \pm 2.5 \mu\text{m}$ and mean length $370 \pm 90 \mu\text{m}$, $n = 248$; finally, order 1 arterioles had mean diameter of $15 \pm 3 \mu\text{m}$ and mean length of $135 \pm 80 \mu\text{m}$, $n = 260$ [29].

Hypoperfusion affected all pial arterioles causing a progressive decrease in their diameters. At end of BCCAO in order 4, 3, and 2 vessels, the reduction was by $20 \pm 3\%$, $18 \pm 2\%$, and $17.5 \pm 3.0\%$ of baseline ($P < 0.01$ versus SO group), respectively (Fig. 2A). The permeability increase was pronounced (0.20 ± 0.03 NGL, $P < 0.01$ versus SO group: 0.04 ± 0.02 NGL) (Fig. 3).

The RE induced arteriolar constriction at the beginning, then dilation, and at 60 min (RE) again constriction by $19.0 \pm 2.8\%$, $12.5 \pm 2.0\%$, and $11.8 \pm 1.2\%$ of baseline in order 4, 3, and 2 arterioles ($P < 0.01$ versus SO group), respectively (Fig. 2B).

The permeability rise was marked on venular side (0.45 ± 0.04 NGL, $P < 0.01$ versus SO group: 0.04 ± 0.02 NGL) as well as adhesion of leukocytes to the venular walls ($8 \pm 2/100 \mu\text{m v.l./30 s}$; $P < 0.01$ versus SO group) (Figs 3 and 4). The PCL was significantly reduced compared with SO group (by $39.2 \pm 6.0\%$ of baseline), while capillary V_{RBC} decreased to 0.15 ± 0.02 mm/s ($P < 0.01$ versus SO group: 0.22 ± 0.03 mm/s).

The animals treated with DCFH-DA superfusion showed an increased DCF fluorescence intensity at the end of BCCAO (0.22 ± 0.02 NGL, $P < 0.01$ versus baseline: 0.03 ± 0.02 NGL), indicating an increase in ROS formation. The fluorescence was higher at RE in the remaining animals (0.30 ± 0.03 NGL, $P < 0.01$ versus baseline) showing a further increase in ROS production.

Melatonin, at the lowest dosage (0.5 mg/kg b.w.), caused a reduction in order 4, 3, and 2 arteriole diameters by $13 \pm 2\%$, $11 \pm 2\%$, and $12.0 \pm 2.2\%$ of baseline ($P < 0.01$ versus C group) and a slight increase in microvascular permeability (0.15 ± 0.02 NGL, $P < 0.01$ versus C group) (Figs 2A and 3).

At RE, order 4 and 3 arteriole diameters were reduced by $4.8 \pm 2.5\%$ and $4.0 \pm 1.7\%$ of baseline, respectively ($P < 0.01$ versus C group), while order 2 vessels presented an increase in frequency of rhythmic diameter changes (0.03 ± 0.01 Hz) compared with baseline (0.02 ± 0.01 Hz)

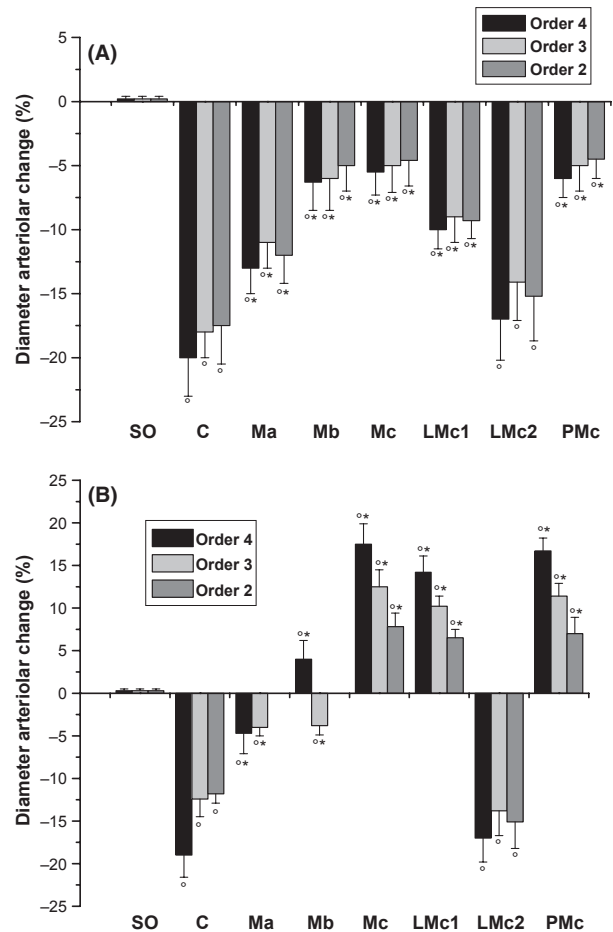


Fig. 2. Diameter changes of order 4, 3, and 2 arterioles, expressed as percentage, at the end of bilateral common carotid artery occlusion (A) and at the end of reperfusion (B) in the experimental groups: SO, sham-operated group ($n = 5$); C, control group; Ma, melatonin 0.5 mg/kg b.w. subgroup ($n = 9$); Mb, melatonin 1.0 mg/kg b.w. subgroup ($n = 9$); Mc, melatonin 2.0 mg/kg b.w. subgroup ($n = 9$); LMc1, luzindole (2.0 mg/kg b.w.) plus melatonin (2.0 mg/kg b.w.) group ($n = 9$); LMc2, luzindole (4.0 mg/kg b.w.) plus melatonin (2.0 mg/kg b.w.) group ($n = 9$); PMc, prazosin (1.0 mg/kg b.w.) plus melatonin (2.0 mg/kg b.w.) group ($n = 9$). The bar lacking indicates presence of rhythmic diameter changes. ° $P < 0.01$ versus SO group, * $P < 0.01$ versus C group.

(Fig. 5A,B). The fluorescence leakage was slightly prevented (0.25 ± 0.03 NGL, $P < 0.01$ versus C group) as well as the leukocyte adhesion ($5 \pm 2/100 \mu\text{m v.l./30 s}$, $P < 0.01$ versus C group) (Fig. 3). Capillary perfusion decreased by $32 \pm 4\%$ and V_{RBC} increased compared with controls (0.26 ± 0.04 mm/s, $P < 0.01$ versus C group).

In rats treated with DCFH-DA, at the end of BCCAO and at RE, NGL were 0.14 ± 0.02 and 0.21 ± 0.03 , respectively ($P < 0.01$ versus C group).

Melatonin, at the intermediate dosage (1.0 mg/kg b.w.), induced arteriole diameter reduction by $6.3 \pm 2.2\%$, $6.0 \pm 2.5\%$, and $5 \pm 2\%$ of baseline in order 4, 3, and 2 arterioles, respectively ($P < 0.01$ versus C group) and NGL were 0.11 ± 0.03 ($P < 0.01$ versus controls) (Figs 2A and 3) at the end of BCCAO.

At RE, each arteriolar order showed a different response. Order 4 arteriole diameters were increased by $4.2 \pm 2.0\%$

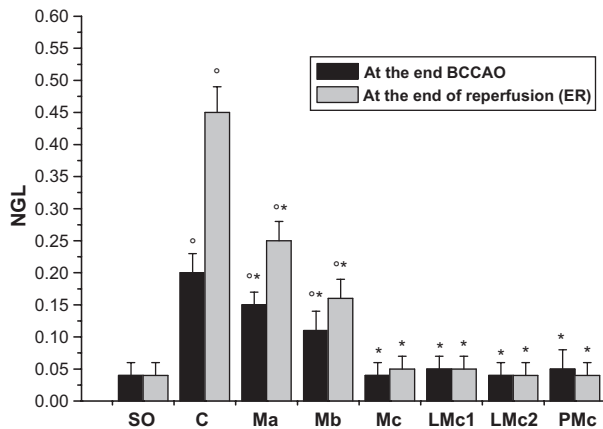


Fig. 3. Permeability increase, expressed as normalized grey levels, after bilateral common carotid artery occlusion (black) and at reperfusion (grey) in the experimental groups: SO, sham-operated group (n = 5); C, control group (n = 9); Ma, melatonin 0.5 mg/kg b.w. subgroup (n = 9); Mb, melatonin 1.0 mg/kg b.w. subgroup (n = 9); Mc, melatonin 2.0 mg/kg b.w. subgroup (n = 9); LMc1, luzindole (2.0 mg/kg b.w.) plus melatonin (2.0 mg/kg b.w.) group (n = 9); LMc2, luzindole (4.0 mg/kg b.w.) plus melatonin (2.0 mg/kg b.w.) group (n = 9); PMc, prazosin (1.0 mg/kg b.w.) plus melatonin (2.0 mg/kg b.w.) group (n = 9). °P < 0.01 versus SO group, *P < 0.01 versus C group.

of baseline ($P < 0.01$ versus C group) and order 3 vessel diameters were reduced by $3.8 \pm 1.2\%$ of baseline, while order 2 arterioles showed a significant increase in frequency of rhythmic diameter changes (0.05 ± 0.02 Hz) compared with baseline (Figs 2B and 5A,C). The microvascular leakage and leukocyte adhesion were prevented (0.16 ± 0.03 NGL and $3 \pm 1/100 \mu\text{m v.l./30 s}$, respectively; $P < 0.01$ versus C group). The capillary perfusion was protected, because the decrease was by $27 \pm 5\%$ of baseline ($P < 0.01$ versus C group) and V_{RBC} increased (0.30 ± 0.03 mm/s, $P < 0.01$ compared with controls).

In rats treated with DCFH-DA, at the end of BCCAO and at RE, NGL were 0.10 ± 0.03 , and 0.16 ± 0.03 ($P < 0.01$ versus controls).

Melatonin at the highest dosage (2.0 mg/kg b.w.) blunted pial arteriolar diameter decrease at the end of BCCAO: order 4, 3, and 2 vessels showed a decrease in diameter by $5.5 \pm 1.8\%$, $5.0 \pm 2.1\%$, and $4.6 \pm 2.0\%$ of baseline, respectively ($P < 0.01$ versus C group) (Fig. 2A). Microvascular permeability was significantly reduced compared with controls (0.04 ± 0.02 NGL, $P < 0.01$ versus C group) (Fig. 3).

At RE, the highest dosage caused an increase in diameter of order 4, 3, and 2 arterioles (by $17.5 \pm 2.5\%$, $12.5 \pm 2.0\%$, and $8.0 \pm 1.5\%$ of baseline, respectively, $P < 0.01$ versus C group) (Fig. 2B) and prevented fluorescent leakage (0.05 ± 0.02 NGL, $P < 0.01$ versus C group) (Fig. 3). Leukocyte adhesion decreased ($2 \pm 1/100 \mu\text{m v.l./30 s}$, $P < 0.01$ versus C group) and capillary perfusion was protected, because the decrease was by $20 \pm 4\%$ of baseline ($P < 0.01$ versus C group), and V_{RBC} increased (0.33 ± 0.03 mm/s, $P < 0.01$ compared with controls).

In rats treated with DCFH-DA, at the end of BCCAO and at RE, NGL were 0.05 ± 0.02 and 0.06 ± 0.03 ,

$P < 0.01$ versus controls, indicating a marked reduction in ROS production when compared with controls.

Finally, melatonin administration (0.5, 1.0, and 2.0 mg/kg b.w.), in rats not subjected to BCCAO and RE, did not affect microvascular parameters when compared with those observed in SO group.

Luzindole, at the lower dosage (2.0 mg/kg b.w.) prior to melatonin (2.0 mg/kg b.w.), partially reduced the effects of melatonin because the diameter of order 4, 3, and 2 arterioles diminished by $10.0 \pm 1.5\%$, $9.0 \pm 2.0\%$, and $9.3 \pm 1.4\%$ of baseline, respectively ($P < 0.01$ versus C group), at the end of BCCAO (Fig. 2A). The permeability increase did not significantly change compared with SO group (Fig. 3).

At RE, pial arterioles showed a slight increase in diameter (by $14.2 \pm 2.0\%$, $10.0 \pm 1.5\%$, and $6.5 \pm 1.0\%$ of baseline, in order 4, 3, and 2 respectively ($P < 0.01$ versus controls) (Fig. 2B). The permeability increase and leukocyte adhesion were prevented as observed in rats treated with the highest dosage of melatonin (Fig. 3). PCL was slightly reduced (by $23 \pm 5\%$ of baseline, $P < 0.01$ versus C group; $P = \text{NS}$ versus Mc subgroup) while V_{RBC} increased (0.25 ± 0.03 mm/s, $P < 0.01$ versus C group; $P = \text{NS}$ versus Mc subgroup).

Luzindole, at the higher dose (4 mg/kg b.w.) prior to melatonin (2 mg/kg b.w.), abolished melatonin-induced effects in order 4, 3, and 2 arterioles: arteriolar diameter decreased by $17.0 \pm 3.2\%$, $14.1 \pm 3.0\%$, and $15.2 \pm 3.5\%$ of baseline, respectively, $P = \text{NS}$ versus controls at the end of BCCAO. Microvascular leakage was prevented as observed in Mc subgroup (Figs 2A and 3).

At RE, luzindole blunted melatonin-induced vasodilation. Pial arterioles constricted by $18.0 \pm 3.5\%$, $13.0 \pm 1.8\%$, and $12.0 \pm 1.5\%$ of baseline in order 4, 3, and 2, respectively ($P = \text{NS}$ versus controls) (Fig. 2B). Leakage and leukocyte adhesion were prevented (0.05 ± 0.03 NGL, $3.0 \pm 1.0/100 \mu\text{m v.l./30 s}$; $P < 0.01$ versus controls) (Fig. 3). PCL decreased by $25 \pm 5\%$ of baseline and V_{RBC} was 0.27 ± 0.03 mm/s, $P < 0.01$ versus controls.

In DCFH-DA-treated animals, NGL were not significantly different when compared with Mc subgroup independently of luzindole dosage utilized.

Luzindole (2.0 and 4.0 mg/kg b.w.), administered prior to BCCAO and at the beginning of RE, did not modify the microvascular responses observed in control rats. Luzindole (2.0 and 4.0 mg/kg b.w.) treatment in animals not subjected to BCCAO and RE did not affect microvascular parameters when compared with those observed in SO group. The luzindole dosages were chosen according to previous data [29].

Prazosin (1.0 mg/kg b.w.) prior to melatonin (2.0 mg/kg b.w.) did not modify the melatonin effects because at the end of BCCAO, order 4, 3, and 2 vessels showed a slight decrease in diameter by $6.0 \pm 1.5\%$, $5.1 \pm 2.0\%$, and $4.5 \pm 1.5\%$ of baseline, respectively ($P < 0.01$ versus C group) (Fig. 2A). Microvascular permeability did not significantly change compared with baseline (Fig. 3). At RE, prazosin plus melatonin caused dilation of order 4, 3, and 2 arterioles (by $16.8 \pm 1.5\%$, $11.5 \pm 1.4\%$, and $7 \pm 2\%$ of baseline, respectively, $P < 0.01$ versus C

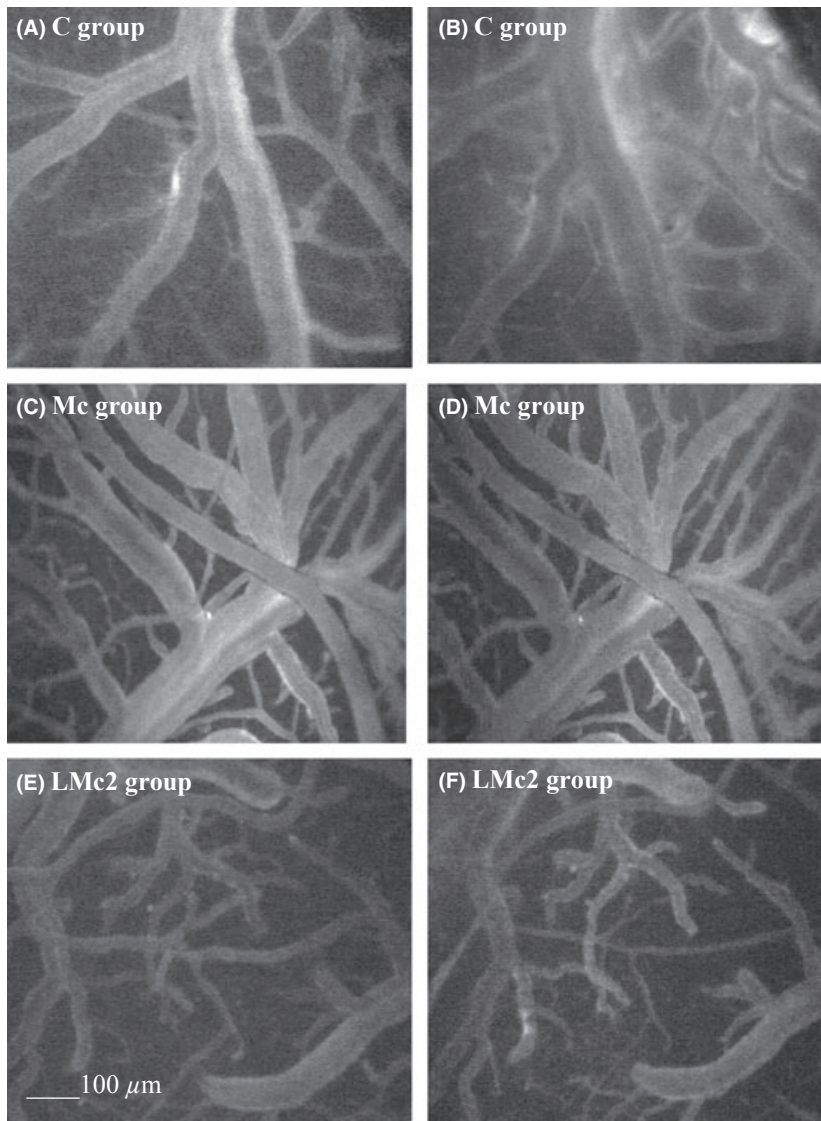


Fig. 4. Computer-assisted image of a pial microvascular network in control rat under baseline conditions (A) and at the end of reperfusion (B); in rat treated with melatonin 2.0 mg/kg b.w. (C, D) and in rat treated with melatonin 2.0 mg/kg b.w. plus luzindole 4.0 mg/kg b.w. (E, F), at the same time points as in control. The increase in permeability is apparent by the marked changes in the colour of interstitium (from black to white). Melatonin or melatonin plus luzindole prevented the increase in permeability because the interstitium did not significantly change in colour (black). Scale bar = $\text{---} 100 \mu\text{m}$.

group) (Fig. 2B). Moreover, microvascular permeability and leukocyte adhesion were prevented as observed in Mc subgroup (Fig. 3). PCL and V_{RBC} did not show significant changes compared with Mc subgroup.

Moreover, in DCFH-DA-treated animals, NGL did not significantly change when compared with Mc subgroup.

Prazosin (1.0 mg/kg b.w.), administered prior to BCCAO and at the beginning of RE, did not significantly modify the microvascular responses, such as those observed in control rats. Prazosin treatment (1.0 mg/kg b.w.) of animals not subjected to BCCAO and RE did not influence microvascular parameters when compared with those observed in SO group. Prazosin dosage was chosen according to previous data [30].

Finally, the physiological parameters, such as hematocrit, MABP, heart rate, pH, PCO_2 , and PO_2 , did not significantly change in the different experimental groups up to RE.

Discussion

Cerebral hypoperfusion triggered by bilateral occlusion of common carotid arteries resulted in arteriolar diameter

reduction and permeability increase. Reperfusion was characterized by marked arteriolar constriction, pronounced microvascular permeability and adhesion of leukocytes, and reduction in capillary perfusion and capillary red blood cell velocity.

Melatonin administered prior to bilateral occlusion of common carotid arteries and at the beginning of RE dose dependently prevented microvascular damage. During BCCAO, melatonin dose dependently prevented arteriolar diameter decrease and leakage. During RE, the lower dosages of melatonin modulated the pial arteriolar tone decreasing the constriction of large arterioles (order 4 and 3), while increasing rhythmic diameter changes in small arterioles (order 2). This oscillation in rat pial arteriolar diameter, defined as vasomotion, has been studied during cortical activation indicating that this phenomenon plays an important role in the regulation of the coupling between neuronal activity and hemodynamic response [31]. Previous studies carried out in different experimental models have shown that rhythmic changes in diameter are able to modulate distribution of blood flow in the terminal

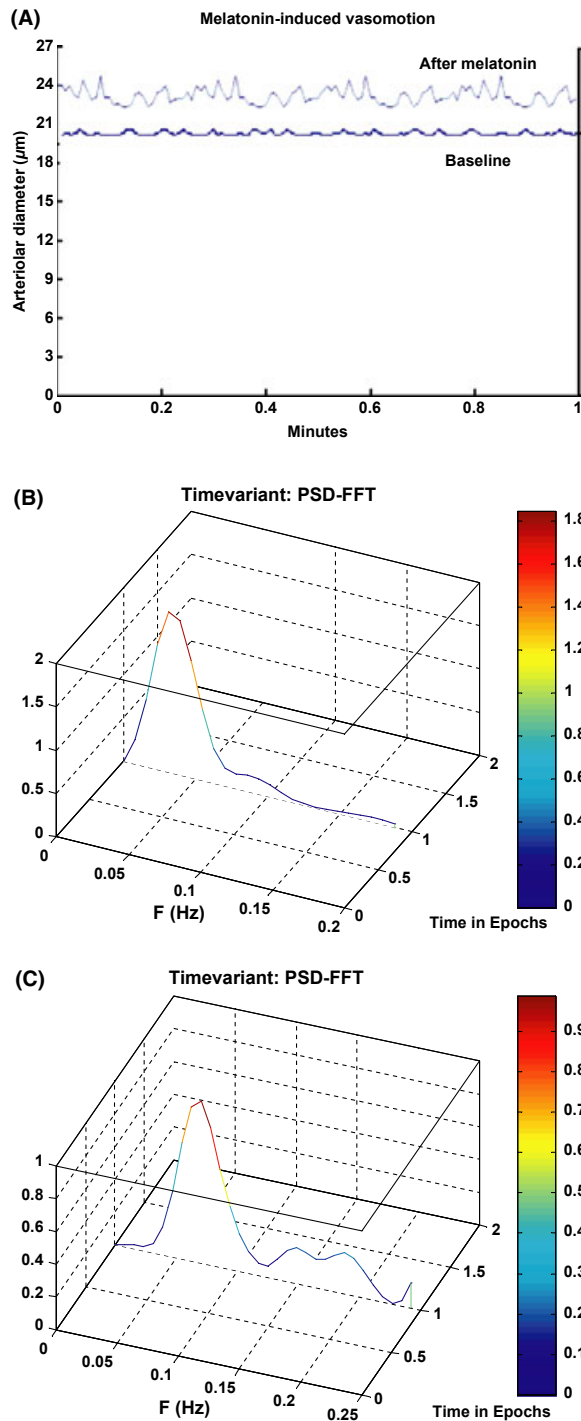


Fig. 5. Rhythmic diameter changes in order 2 arteriole of a rat under baseline conditions (down) and after treatment with melatonin (1 mg/kg b.w., Mb subgroup) (upper) (A). Corresponding power spectra under baseline conditions (B) and after treatment with melatonin (1 mg/kg b.w., Mb subgroup) (C). PSD: power spectral density ($\mu\text{m}^2/\text{Hz}$).

arteriolar branchings [32]. Our data indicate that low-dose melatonin increased the arteriolar oscillation frequency during RE, likely improving blood flow distribution in microvascular networks and consequently cerebral tissue oxygenation.

The highest dose of melatonin caused dilation of all arteriolar orders. These results are in agreement with the data reported by Régrigny and coworkers [19], who demonstrated that melatonin's topical application (at low dosage) induces vasoconstriction of pial large arteries (mean diameter $>60 \pm 4 \mu\text{m}$) while small pial arterioles dilate. Furthermore, our data indicate that melatonin dose dependently prevented microvascular permeability and leukocyte adhesion, and preserved capillary perfusion and capillary red blood cell velocity.

Luzindole administration prior to melatonin caused different arteriolar responses at the different dosages. Luzindole at the lower dosage caused partial inhibition of melatonin-induced dilation, while the higher dosage completely abolished the melatonin-triggered vasodilation causing pronounced arteriolar diameter reduction as observed in control animals. Luzindole did not affect the protective effects of melatonin on BCCAO and RE-induced injuries, such as leakage and leukocyte adhesion. Previous *in vitro* study carried out in rats indicate that lower dosage of luzindole inhibits MT2 melatonin receptors, while higher dosage inhibits MT1 and MT2 melatonin receptors [33].

The data of the present study suggest that melatonin modulates the pial arteriole tone during hypoperfusion and RE. Melatonin activates MT1 and MT2 receptors; it is possible to suggest that the lower dosage of melatonin activated MT2 receptors, while the higher dosage of melatonin was able to stimulate also MT1 receptors. However, the stimulation of MT2 melatonin receptors induced rhythmic diameter changes in smaller arterioles, contributing to the microvascular blood flow regulation during ischemia-RE. However, melatonin exhibited further effects preventing microvascular injuries. This protection was independent of MT1 and MT2 melatonin receptor activation. These effects are probably due to antioxidant activity as indicated by our data in DCFH-DA-treated animals.

MT3 melatonin receptor inhibition by prazosin did not alter melatonin-induced protective effects during hypoperfusion and RE. MT3 melatonin receptor is a quinone reductase two whose intracellular signaling pathway has not been fully clarified. It was suggested that MT3 melatonin receptors may contribute to melatonin antioxidant properties [34]. Our data confirm melatonin scavenger activity, but prazosin administration did not interfere with melatonin antioxidant effects. These results are supported by reports documenting the ability to detoxify free radicals and related oxygen derivatives by melatonin is likely due to a receptor-independent pathway [35].

In conclusion, it is reasonable to suggest that melatonin's protective mechanisms against brain ischemia-RE injury may be because of different actions. Melatonin modulates the arteriolar tone promoting an efficient redistribution of microvascular blood flow; this activity is mediated by MT1 and MT2 melatonin receptors. Moreover, melatonin has a powerful scavenger activity against the oxygen-derived free radicals with slight or no involvement of MT3 melatonin receptors. All these properties contribute to melatonin's effects that appear to ameliorate brain ischemia and RE damages.

References

1. TAN DX, CHEN LD, POEGGELER B et al. Melatonin: a potent, endogenous hydroxyl radical scavenger. *Endocr J* 1993; **1**:57–60.
2. HARDELAND R, TAN DX, REITER RJ. Kynuramines, metabolites of melatonin and other indoles: the resurrection of an almost forgotten class of biogenic amines. *J Pineal Res* 2009; **47**:109–126.
3. CHEUNG RTF. The utility of melatonin in reducing cerebral damage resulting from ischemia and reperfusion. *J Pineal Res* 2003; **34**:153–160.
4. CERVANTES M, MORALI G, LETECHEPIA-VALLEJO G. Melatonin and ischemia-reperfusion injury of the brain. *J Pineal Res* 2008; **45**:1–7.
5. PARADIES G, PETROSILLO G, REITER RJ et al. Melatonin, cardiolipin and mitochondrial bioenergetics in health and disease. *J Pineal Res* 2010; **48**:297–310.
6. LI XY, ZHANG LM, GU J et al. Melatonin decreases production of hydroxyl radical during cerebral ischemia-reperfusion. *Zhongguo Yao Li Xue Bao* 1997; **18**:394–396.
7. GITTO E, PELLEGRINO S, D'ARRIGO S et al. Oxidative stress in resuscitation and in ventilation of newborns. *Eur Respir J* 2009; **34**:1461–1469.
8. JOU MJ, PENG TI HSU LF, HSU LF et al. Visualization of melatonin's multiple mitochondrial levels of protection against mitochondrial Ca(2+)-mediated permeability transition and beyond in rat brain astrocytes. *J Pineal Res* 2010; **48**:20–38.
9. PEI Z, FUNG PC, CHEUNG RT. Melatonin reduces nitric oxide level during ischemia but not blood-brain barrier breakdown during reperfusion in a rat middle cerebral artery occlusion stroke model. *J Pineal Res* 2003; **34**:110–118.
10. MANEV H, UZ T. Primary cultures of rat cerebellar granule cells as a model to study neuronal 5-lipoxygenase and FLAP gene expression. *Ann NY Acad Sci* 1999; **890**:183–190.
11. SINHA K, DEGAONKAR MN, JAGANNATHAN NR et al. Effect of melatonin on ischemia reperfusion injury induced by middle cerebral artery occlusion in rats. *Eur J Pharmacol* 2001; **428**:185–192.
12. KONDOH T, UNEYAMA H, NISHINO H et al. Melatonin reduces cerebral edema formation caused by transient forebrain ischemia in rats. *Life Sci* 2002; **72**:583–590.
13. CUZZOCREA S, COSTANTINO G, GITTO E et al. Protective effects of melatonin in ischemic brain injury. *J Pineal Res* 2000; **29**:217–227.
14. TORII K, UNEYAMA H, NISHINO H et al. Melatonin suppress cerebral edema caused by middle cerebral artery occlusion/reperfusion in rats assessed by magnetic resonance imaging. *J Pineal Res* 2004; **36**:18–24.
15. REITER RJ, PAREDES SD, MANCHESTER LC et al. Reducing oxidative/nitrosative stress: a newly-discovered genre for melatonin. *Crit Rev Biochem Mol Biol* 2009; **44**:175–200.
16. WITT-ENDERBY PA, BENNETT J, JARZYNSKA MJ et al. Melatonin receptors and their regulation: biochemical and structural mechanisms. *Life Sci* 2003; **72**:2183–2198.
17. VON GALL C, STEHLE JH, WEAVER DR. Mammalian melatonin receptors: molecular biology and signal transduction. *Cell Tissue Res* 2002; **309**:151–162.
18. RÈGRIGNY O, DELAGRANGE P, SCALBERT E et al. Melatonin increases pial artery tone and decreases the lower limit of cerebral blood flow autoregulation. *Fundam Clin Pharmacol* 2001; **15**:233–238.
19. RÈGRIGNY O, DELAGRANGE P, SCALBERT E et al. Effects of melatonin on rat pial arteriolar diameter in vivo. *Br J Pharmacol* 1999; **127**:1666–1670.
20. GEARY GG, KRAUSE DN, DUCKLES SP. Melatonin directly constricts rat cerebral arteries through modulation of potassium channels. *Am J Physiol* 1997; **273**:H1530–H1536.
21. NGAI AC, KO KR, MORII S et al. Effect of sciatic nerve stimulation on pial arterioles in rats. *Am J Physiol* 1988; **254**:H133–H139.
22. MORII S, NGAI AC, WINN R. Reactivity of rat pial arterioles and venules to adenosine and carbon dioxide: with detailed description of the closed cranial window technique in rats. *J Cereb Blood Flow Metab* 1986; **6**:34–41.
23. HUDETZ AG, FEHER G, WEIGLE CGM et al. Video microscopy of cerebrocortical capillary flow: response to hypotension and intracranial hypertension. *Am J Physiol* 1995; **268**:H2202–H2210.
24. GOLANOV EV, YAMAMOTO S, REIS DJ. Spontaneous waves of cerebral blood flow associated with a pattern of electrocortical activity. *Am J Physiol* 1994; **266**:R204–R214.
25. LAPI D, MARCHIAFAVA PL, COLANTUONI A. Geometric characteristics of arterial network of rat pial microcirculation. *J Vasc Res* 2008; **45**:69–77.
26. COLANTUONI A, LAPI D, PATERNI M et al. Protective effects of insulin during ischemia-reperfusion injury in hamster cheek pouch microcirculation. *J Vasc Res* 2005; **42**:55–66.
27. SCARGLE JD. Statistical aspects of spectral analysis of unevenly spaced data. *Astrophys J* 1982; **263**:835–853.
28. WATANABE S. In vivo fluorometric measurement of cerebral oxidative stress using 2'-7'-dichlorofluorescein (DCF). *Keio J Med* 1998; **47**:92–98.
29. MATHES AM, KUBULUS D, WAIBEL L et al. Selective activation of melatonin receptors with ramelteon improve liver function and hepatic perfusion after hemorrhagic shock in rat. *Crit Care Med* 2008; **36**:2863–2870.
30. YU CX, ZHU CB, XU SF et al. Selective MT(2) melatonin receptor agonist blocks melatonin-induced antinociception in rats. *Neurosci Lett* 2000; **282**:161–164.
31. VETRI F, MENICUCCI D, LAPI D et al. Pial arteriolar vasomotion changes during cortical activation in rats. *Neuroimage* 2007; **38**:25–33.
32. BERTUGLIA S, COLANTUONI A, COPPINI G et al. Hypoxia or hyperoxia induced changes in arteriolar vasomotion in skeletal muscle microcirculation. *Am J Physiol* 1991; **260**:H362–H372.
33. DUBOCOVICH ML. Melatonin receptors: are there multiple subtypes?. *Trends Pharmacol Sci* 1995; **16**:50–56.
34. BOUSSARD MF, TRUCHE S, ROUSSEAU-ROJAS A et al. New ligands at the melatonin binding site MT3. *Eur J Med Chem* 2006; **41**:306–320.
35. REITER RJ, TAN DX, FUENTES-BROTO L. Melatonin: a multitasking molecule. *Prog Brain Res* 2010; **181**:127–151.